

Doped Keggin heteropolyacids as catalysts in sulfide oxidation

Valeria Palermo · Ángel G. Sathicq ·
Patricia G. Vázquez · Horacio J. Thomas ·
Gustavo P. Romanelli

Received: 2 February 2011 / Accepted: 6 June 2011 / Published online: 25 June 2011
© Akadémiai Kiadó, Budapest, Hungary 2011

Abstract In this research, we report the preparation of doped PMo Keggin heteropolyacids where Mo is partially replaced by V, Bi, and Bi–V. These catalysts were characterized by means of ICP-AES analysis, ^{31}P -NMR, UV–visible spectra, FT-IR spectra, thermal analysis, and textural properties. In addition, the activities of the synthesized catalysts were evaluated in the selective oxidation of sulfides to sulfoxides/sulfones. The incorporation of V, Bi and Bi–V into the structure of $\text{H}_3\text{PMo}_{12}\text{O}_{40}$ increases the catalytic activity. The two most active catalysts, those with V and V–Bi were supported on aminopropyl-functionalized silica (SiO_2NH_2) and they were found to be and efficient heterogeneous catalysts for the selective oxidation of diphenylsulfide to the corresponding sulfoxide/sulfone.

Keywords Doped Keggin heteropolyacids · Sulfide oxidation · Bulk and supported catalysts · Sulfoxides · Sulfones

Introduction

Heteropolyacids (HPAs) are transition metal–oxygen anion clusters that exhibit a wide range of molecular sizes, compositions, and architectures [1].

There is an increasing interest in the area of heteropolycompound-induced organic transformations. In view of their remarkable catalytic properties, heteropolycompounds are applied both in bulk or supported form, and homogeneous or heterogeneous catalysis is possible.

V. Palermo · Á. G. Sathicq · P. G. Vázquez · H. J. Thomas · G. P. Romanelli (✉)
Centro de Investigación y Desarrollo en Ciencias Aplicadas “Dr. Jorge J. Ronco” (CINDECA),
CCT-LaPlata-CONICET, Facultad de Ciencias Exactas, Universidad Nacional de La Plata,
47 N° 257 (B1900AJK) La Plata, Argentina
e-mail: gpr@quimica.unlp.edu.ar

Heteropolyacids have been used in a variety of acid-catalyzed reactions such as esterification, etherification, olefin hydration, and dehydration of alcohols, and are also attractive as catalysts for oxidation processes [2]. Recently, we have used Keggin heteropolyacids in a range of processes, i.e., preparation of heterocycles [3, 4], protection/deprotection of organic functional groups [5, 6] and oxidation processes, as well as substituted phenol, alcohol and amine oxidation, and the selective oxidation of sulfides to sulfoxides with aqueous H_2O_2 [7–9].

Vanadium incorporated molybdophosphoric acid ($\text{H}_4\text{PMo}_{11}\text{VO}_{40}$) shows unique catalytic features for oxidation due to its bi-functional character, which arises because of the redox nature of vanadium and the oxidation/acidic character of the molybdophosphoric acid ($\text{H}_3\text{PMo}_{12}\text{O}_{40}$, PMo) catalysts by replacing Mo atoms with the corresponding V atoms. These heteropolycompounds are studied due to their importance as catalysts in catalytic oxidation reactions, for example, the hydroxylation of benzene, the oxidation of toluene, nitrobenzene and norbornene using aqueous hydrogen peroxide [10], benzyl alcohol oxidation [11], benzoin oxidation to benzyls, aldehydes and esters by dioxygen [12], and liquid-phase oxidation of methane with hydrogen peroxide [13].

On the other hand, the selective oxidation of sulfides is of interest because of the importance of sulfoxides and sulfones as synthetic intermediates in organic synthesis.

Sulfoxides are important in organic synthesis as an activating group; they have been used extensively in carbon bond-forming reactions [14] as building blocks, especially as chiral auxiliaries [15], and they play key roles in enzyme activation [16]. Sulfones and their derivatives are widely applied. They can be used as intermediates for pharmaceuticals and pesticides, and for the modification of polymers [17, 18]. Certain sulfones are effective herbicides and others act as insecticides, and acaricides [19]; certain heterocyclic sulfones can be used as corrosion protection agents for metals [20].

There are several reagents available for these key transformations; they are conventionally achieved using stoichiometric amounts of both organic and inorganic reagents, for example, nitric acid, chromic acid, manganese dioxide, ozone, sodium periodate, selenium dioxide, hypervalent iodine reagents, sodium-perborate/sodium perborate [21], halogen [22], and binuclear manganese complex-periodic acid [23].

During the last decade, very useful procedures involving catalysis and hydrogen peroxide as oxidant, for example, H_2WO_4 , $\text{H}_3\text{PW}_{12}\text{O}_{40} + [(\text{C}_8\text{H}_{17})_4\text{N}]\text{Br}$, Rhenium (V) oxo-phosphine complexes, methyltrioxorhenium, Sc (OTf)₃, (salem) Mn (III), and Ti (IV) complexes, Tellurium dioxide and $\text{TPPF}_e(\text{III})\text{Cl}$ -imidazole, have been used [24]. They have been developed to promote the oxidation of organic substrates due to their effective oxygen content, low cost, and safety in storage and operation [25, 26].

In this study, we report the preparation of doped Keggin structures where Mo is partially replaced by V, Bi, and Bi–V, respectively, in the primary structure of PMo. The activities of the synthesized catalysts were evaluated in the selective oxidation of sulfides to sulfoxides, using aqueous hydrogen peroxide as oxidant. Two bulk HPAs (those doped with V and VBi) were supported on aminopropyl-functionalized silica (SiO_2NH_2) and they were prepared by the equilibrium adsorption technique. These catalysts were well characterized by means of ^{31}P -NMR, UV–visible spectra,

FT-IR spectra, thermal analysis, and textural properties. Mo, V and Bi amounts were estimated by ICP-AES analysis.

Experimental

Catalyst synthesis

Heteropolyacid synthesis. Bulk heteropolyacid synthesis

The catalysts were prepared by the hydrothermal synthesis method [27]. The following HPA synthesis procedure was used: a stoichiometric mixture of MoO_3 , the corresponding metal oxide and H_3PO_4 [85% (w/v)] were suspended in 120 mL of distilled water. The mixture was stirred for 3 h at 75 °C. After cooling down to room temperature and removal of insolubles, the heteropolyacid solution was evaporated and dried at 40 °C. Colorful crystals of pure catalysts were obtained. The used nomenclature was: -doped with V: PMoV, -doped with Bi: PMoBi, and -doped with V–Bi: PMoVBi.

The experimental contents of Mo, V and Bi in the bulk HPA were determined by means of the inductively coupled plasma atomic emission spectroscopy (ICP-AES) technique using a Shimadzu 1000 III instrument.

Supported PMoV, and PMoBiV synthesis. Silica preparation via sol–gel technique

Tetraethoxysilane (TEOS) (102 mL), absolute ethanol (99.99%) (42 mL), and glacial acetic acid (30 mL), in a molar ratio equal to 1:1.6:1.1, were mixed in a glove box under nitrogen atmosphere at room temperature. The mixture was removed from the controlled atmosphere and another part of absolute ethanol (90 mL) was added, and then sol gelation took place. Finally, wet gel was aged in the same medium until dry silica particles were obtained. These particles were dried at room temperature and this solid was named SiO_2 [specific surface area (S_{BET}): 292.1 m^2/g].

Preparation of functionalized silica

SiO_2 (4 g) was refluxed with toluene (128 mL) for 1 h. Then, 3-aminopropyltrimethoxysilane (APS) (6.40 mL) was added and stirred under reflux conditions for 24 h. The solid was filtered, washed in a Soxhlet apparatus with diethyl ether and dichloromethane and dried at 40 °C according to Ref. [28]. These particles were dried at 40 °C and this solid was named SiO_2NH_2 [the specific surface area (S_{BET}) near of about 2 m^2/g , this value is low and near to experimental error], and the $-\text{NH}_2$ content was estimated to be near 3.5 mmol per g of SiO_2 .

Preparation of silica-supported catalysts

Supported catalysts were obtained by the equilibrium adsorption technique. The solutions for impregnation were prepared by dissolution of the HPAs (PMoV and

PMoVBi, 160 mg of each one) in absolute ethanol (3.50 mL). The first step in the impregnation technique was to contact the HPA solution with the support SiO_2NH_2 (500 mg), with addition of H_2O (0.50 mL). The support with impregnated solution was left in contact during 24 h.

The two new catalysts were named $\text{SiO}_2\text{NH}_2\text{PMoV}$ and $\text{SiO}_2\text{NH}_2\text{PMoVBi}$. The final contents of HPAs in the catalysts $\text{SiO}_2\text{NH}_2\text{PMoV}$ and $\text{SiO}_2\text{NH}_2\text{PMoVBi}$ were 24.5 and 23.8% (w/w), respectively.

Catalyst characterization

Inductively coupled plasma atomic emission spectroscopy (ICP-AES)

The experimental contents of Mo, V and Bi in the bulk HPA were determined by means of the inductively coupled plasma atomic emission spectroscopy (ICP-AES) technique using a Shimadzu 1000 III instrument.

^{31}P nuclear magnetic resonance (^{31}P -NMR)

Solid samples were analyzed by ^{31}P MAS NMR by means of Varian Mercury Plus 300 equipment with a sample holder 7 mm in diameter, a resonance frequency of 121.469 MHz, and a spinning rate 5 kHz. The measurements were carried out at room temperature using 85% (w/v) H_3PO_4 as external reference.

UV-visible spectroscopy (UV-VIS)

UV-visible spectra of solutions in quartz cuvettes were measured at room temperature with a Perkin Elmer Lambda 35 UV-vis double beam spectrophotometer, in the range 200–1,100 nm. This spectrometer uses tungsten and deuterium lamps to provide visible and UV wavelengths. Ethanolic solutions of 0.001 M concentration were chosen, and all samples were soluble at this concentration. The adsorption edge for each compound was defined by extrapolating the region of steep descent in the spectrum to zero, as shown in Fig. 1 for $\text{H}_3\text{PMo}_{12}\text{O}_{40}$, using the method reported by Barteau et al. [29].

Fourier transform infrared spectroscopy (FT-IR)

Thermo Nicolet IR.200 equipment, pellets in BrK, and a measuring range of 400–4,000 cm^{-1} were used to obtain the FT-IR spectra of the solid samples at room temperature.

Textural properties

Specific surface area (S_{BET}): the pore volume and the mean pore diameter of the supported catalysts were determined by nitrogen adsorption/desorption techniques using Micromeritics ASAP 2020 equipment at liquid-nitrogen temperature. The sample was previously degassed at 100 °C for 1 h.

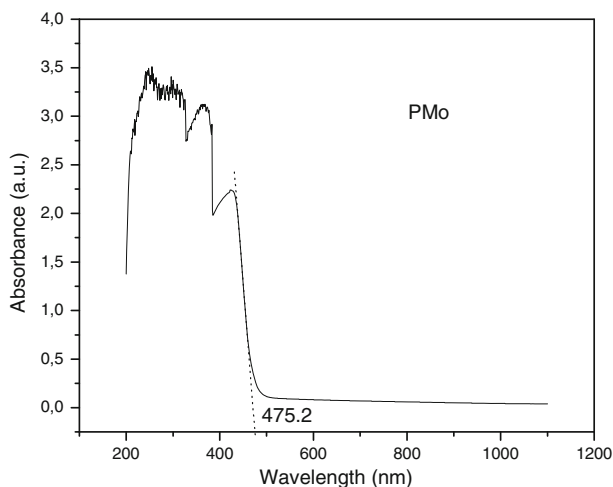


Fig. 1 UV-visible spectrum of 0.001 M ethanolic solution of PMo

Catalytic activity test

General

All reagents were purchased from Merck and Aldrich and used without further purification. All yields refer to isolated products after purification. The products were characterized by spectroscopy data (^1H and ^{13}C -NMR). The NMR spectra were recorded on a 200 MHz Bruker spectrometer. The NMR spectra were measured in CDCl_3 relative to TMS (0.00 ppm). The organic phase was dried on anhydrous Na_2SO_4 and filtered for its analysis by gas chromatography using Varian Scan 3400 cx equipment. The product distribution was quantified by a Shimadzu C-R34 instrument. Reactions were monitored by thin layer chromatography (TLC) analyses.

Diphenylsulfide oxidation

Under homogeneous conditions

Selective oxidation of diphenylsulfide to diphenylsulfoxide Bulk HPA (6 mg, ~ 0.003 mmol), diphenylsulfide (0.5 mmol, 93 mg), and ethanol (2 mL) were stirred at 25 °C. Then aqueous H_2O_2 , 35% (w/v) (0.65 mmol, 0.075 mL), was added. The progress of the reaction was monitored by TLC and GC-MS analysis. After the end of the reaction, it was treated with dichloromethane (10 mL) and water (2×3 mL). The organic phase was dried on anhydrous Na_2SO_4 and concentrated to obtain diphenylsulfoxide. The molar ratio between diphenylsulfide and H_2O_2 35% (w/v) was 1:1.3.

Selective oxidation of diphenylsulfide to diphenylsulfone Diphenylsulfone was obtained using bulk HPAs (12 mg, ~ 0.006 mmol), diphenylsulfide (1 mmol, 186 mg), 35% (w/v) H_2O_2 (6.60 mmol, 0.70 mL), and ethanol (4 mL) at 50 °C.

The molar ratio between diphenylsulfide and H_2O_2 35% (w/v) was 1:6.6.

Under heterogeneous conditions

Selective oxidation of diphenylsulfide to diphenylsulfoxide The supported catalyst (25 mg), diphenylsulfide (0.5 mmol, 93 mg), and ethanol (2 mL) were stirred at 25 °C. Then 35% (w/v) H_2O_2 (0.65 mmol, 0.075 mL) was added. The progress of the reaction was monitored by TLC and GC–MS analysis. After the end of the reaction, the catalyst was recovered by centrifugation and washed with dichloromethane (10 mL). The reaction mixture was treated with dichloromethane (10 mL) and water (2×3 mL). The organic phase was dried on anhydrous Na_2SO_4 and concentrated to obtain diphenylsulfoxide.

The molar ratio between diphenylsulfide and H_2O_2 35% (w/v) was 1:1.3.

Selective oxidation of diphenylsulfide to diphenylsulfoxide or diphenylsulfone Diphenylsulfone was obtained similarly using 0.375 mL of H_2O_2 35% (w/v) at 50 °C.

The molar ratio between diphenylsulfide and H_2O_2 35% (w/v) was 1:6.5.

Recycling of catalyst After reaction, the catalyst was filtered, washed with ethanol, dried under vacuum, and reused for the next cycle of oxidation reaction, following the procedure described above.

Results and discussion

Catalysis characterization

The experimental contents of Mo, V and Bi in the bulk HPA were determined by means of the inductively coupled plasma atomic emission spectroscopy (ICP–AES) technique using a Shimadzu 1000 III instrument. The analysis of the prepared heteropolyacids is as follows:

$\text{H}_4\text{PMo}_{11}\text{VO}_{40} \cdot 12\text{H}_2\text{O}$. Calculated (theoretical): Mo, 52.83, V, 2.55. Found: Mo, 52.85, V 3.4.

$\text{H}_6\text{PMo}_{11}\text{O}_{40}\text{BiO}_{40} \cdot 12\text{H}_2\text{O}$. Calculated (theoretical): Mo, 46.96, Bi, 9.30. Found: Mo, 47.45, Bi, 9.36.

$\text{H}_5\text{PMo}_{11}\text{V}_{0.5}\text{Bi}_{0.5} \cdot 12\text{H}_2\text{O}$. Calculated (theoretical): Mo, 50.92, V 1.23, Bi, 5.04. Found: Mo, 50.55, V 3.51, Bi 0.16.

The experimental results show some deviations of the calculated values. This is due to possible formation of a mixture of compounds during the one-pot synthesis. For example, PMoV contains a higher amount of vanadium than the expected, which indicates the presence as the admixture of $\text{H}_5\text{PV}_2\text{M}_{10}\text{O}_{40}$. Similarly, for the PMoVBi catalyst, the elemental composition corresponds to the probable formation of $\text{H}_4\text{PVMo}_{11}\text{O}_{40}$ with a little higher admixture of $\text{H}_5\text{PV}_2\text{Mo}_{10}\text{O}_{40}$ than in the first case, and of a small amount of a separate PMoBi compound.

The results obtained by ^{31}P -MAS-NMR are listed in Table 1. All the chemical shifts appear at higher magnetic fields than that of the external reference used (H_3PO_4). The spectrum of bulk PMo has one sharp line at -3.61 ppm. A similar

Table 1 ^{31}P -MAS NMR spectra and absorption edge energies of PMo, PMoV, PMoBi and PMoVBi

Entry	Catalyst	^{31}P -NMR MAS (δ ppm)	Edge energy (E) ^a (eV)
1	PMo	-3.61	2.68
2	PMoV	-3.2	2.31
3	PMoBi	-3.64	2.59
4	PMoVBi	-3.17	2.26

^a Edge energy (E) was calculated from the absorption edge wavelength by $E = hc/\lambda$, where h is Planck's constant and c is the speed of light

result was obtained for PMoBi (-3.64 ppm) and PMoV and PMoBiV have one sharp line at -3.20 and 3.17, respectively [30].

Fig. 1 shows UV-visible spectra of the bulk PMo solutions. The band attributed to oxygen-metal transfers at 210–260 nm can be seen in all the spectra. Moreover, Table 1 includes all the absorption edges of HPAs measured in this study. The introduction of V into the framework of Keggin ion heteropolyacids results in lower absorption edge energies in UV-visible spectra. This property is conserved when Bi and V are included during HPA synthesis. But when Bi is only incorporated in the synthesis, the absorption edge energy is near that of PMo.

The results obtained by FT-IR spectra of bulk HPAs are shown in Fig. 2. The vibration spectra of the bulk HPAs with Keggin structure are modified as a function of the nature of the elements introduced into their structure. The FT-IR spectrum of PMo has been previously studied [31], the main bands were observed at 1,064 (P-O_a), 962 (Mo-O_d), 871 (Mo-O_b-Mo), and 780 (Mo-O_c-Mo) cm⁻¹. In the FT-spectrum of PMoV, bands at 1,061 with a shoulder at 1,081 (P-O_a), 960 (Mo-O_d), 863 (Mo-O_b-Mo), and 777 (Mo-O_c-Mo) cm⁻¹ were observed, as reported by Villabrille and coworkers [30]. In the FT-IR spectrum of PMoBi the main bands were observed at 1,063 (P-O_a), 966 (Mo-O_d), 872 (Mo-O_b-Mo), and 789 (Mo-O_c-Mo) cm⁻¹, and in PMoBiV the principal bands were observed at 1,061 (P-O_a), 962 (Mo-O_d), 865 (Mo-O_b-Mo), and 780 (Mo-O_c-Mo) cm⁻¹. When another atom is introduced into the PMo structure, the same characteristic bands are present in the spectra, which confirm the Keggin structure, but the difference in length of the bonds could be introducing defects into the original spectrum. Here it is important to consider the atomic properties of V and Bi. Although the small displacements that take place in some bands (Fig. 2), as shown for Mo-O_b-Mo, could be due to many different reasons during the incorporation of V, Bi or V-Bi into the structure, they are usually attributed to vibrations of the bridges between “inter” (Mo-O_b-Mo) and “intra” (Mo-O_c-Mo) groups (Mo₃O₁₃).

For a better definition of the species resulting from the interaction of both heteropolyacids with the impregnated support in equilibrium, they were characterized by FT-IR. In Fig. 3, FT-IR spectra of the functionalized support (SiO₂NH₂), bulk PMoV and PMoBiV, and supported catalysts (SiO₂NH₂PMoV) and (SiO₂NH₂PMoBiV) are shown. The characteristic spectrum of silica shows bands at 1,000, 800, and 470 cm⁻¹; there are other bands at 3,400 and 1,620 cm⁻¹ attributed to the stretching and bending of the OH groups, respectively [32]. In

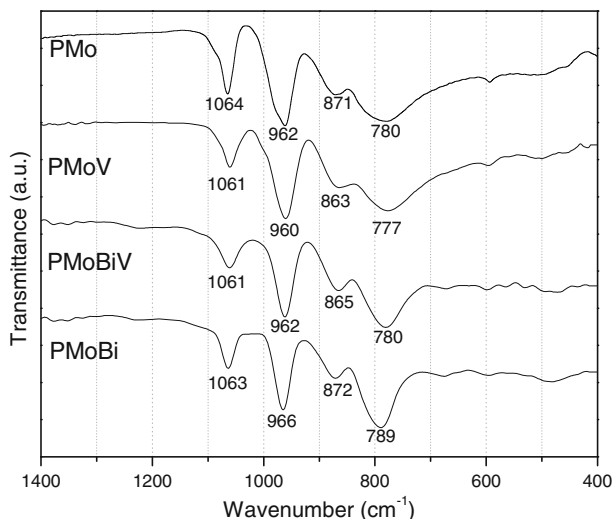


Fig. 2 FT-IR spectra of bulk PMo, PMoV, PMoBiV and PMoBi catalysts

relation to functionalized silica, the main differences are the N–H stretching (band $3,300\text{--}2,600\text{ cm}^{-1}$) broad peak overlapped with the silanol stretching bands of silica and $-\text{CH}_2-$ groups. The small shoulders at the $3,000\text{--}2,750\text{ cm}^{-1}$ region can be assigned to C–H stretching of the amino propyl group at the silica surface. Also, the functionalizing agent (APS) used in the grafting process presents a strong band at the $1,110\text{--}1,050\text{ cm}^{-1}$ region attributed to Si–O–C aliphatic groups, which is observed as a transmittance increase of the silica band in the functionalized support. In addition, the APS band at 790 cm^{-1} is present without overlapping and a transmittance increase at 550 cm^{-1} can be seen on the silica band [33].

During the equilibrium impregnation technique, there is an electrostatic interaction between amino groups and bulk HPAs. By this characterization technique it is very difficult to obtain a band corresponding to PMoV due to overlapping with other bands of the support.

N_2 adsorption tests were used to give a textural characterization of the catalysts and the results [S_{BET} (m^2/g)] are listed in Table 2. The S_{BET} areas for bulk HPAs are low, between 2.7 and $13.8\text{ m}^2/\text{g}$ (Table 2, entry 1–4). Supported catalysts $\text{SiO}_2\text{NH}_2\text{PMoV}$ and $\text{SiO}_2\text{NH}_2\text{PMoVBi}$ show a slightly lower surface area ($4.4\text{ m}^2/\text{g}$). This effect can be attributed to an electrostatic interaction between NH_2 groups and HPA proton, as mentioned in the previous paragraph, due to an umbrella effect of APS [33] on silica, and then the specific surface area is reduced for bulk HPA impregnation.

Catalytic test

Selective oxidation of diphenylsulfide

Initially, the catalytic performances of the different bulk synthesized heteropolyacids (PMoV, PMoBi, and PMoVBi) were evaluated in a homogeneous oxidation

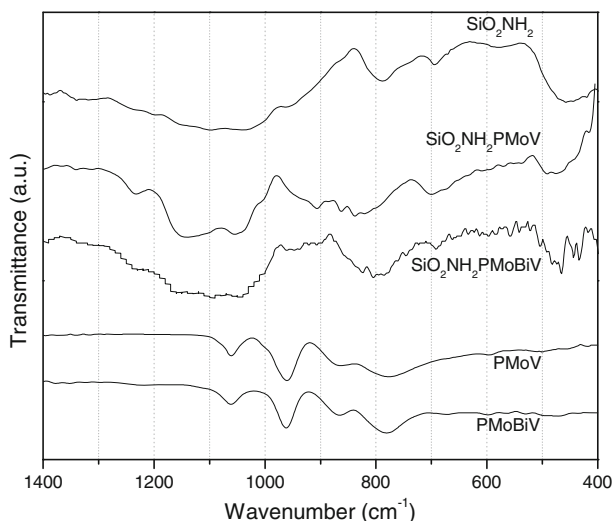


Fig. 3 FT-IR spectra of supported $\text{SiO}_2\text{-NH}_2\text{-PMoV}$ and $\text{SiO}_2\text{-NH}_2\text{-PMoBiV}$ catalysts

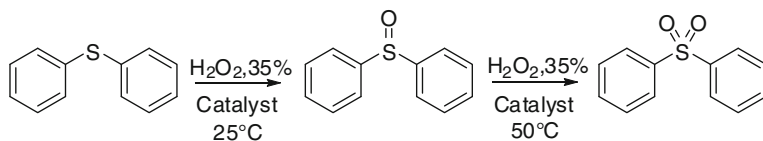
Table 2 S_{BET} (m^2/g) values of HPA catalysts

Entry	Samples	S_{BET} (m^2/g)
1	PMo	12.1
2	PMoV	13.8
3	PMoBi	2.7
4	PMoVBi	6.8
5	$\text{SiO}_2\text{NH}_2\text{PMoV}$	4.4
6	$\text{SiO}_2\text{NH}_2\text{PMoVBi}$	4.4

reaction. The oxidation of diphenylsulfide with aqueous hydrogen peroxide [35% (w/v)] was selected as the model reaction (Scheme 1). Ethanol was chosen as the solvent of the reaction because it gives a homogeneous phase with the reagents and it is a nontoxic and safe solvent.

We first screened the selective oxidation of diphenylsulfide to diphenylsulfoxide using the different catalysts. The blank experiment was performed in the absence of the catalyst using an almost stoichiometric amount of aqueous H_2O_2 (35% (w/v), 0.075 mL, 0.78 mmol). Under these conditions, the reaction conversion was very low (5% for 7 h), at 25 °C (Fig. 4), but when an HPA is added, the conversion increases to values between 58 and 75%.

For these conditions, PMoV and PMoBiV showed the best performance. When PMoV was used, a conversion of 74% was observed at 7 h, with 94% of sulfoxide selectivity. Similarly, PMoVBi showed a conversion and selectivity of 75 and 90%, respectively, in this time period. Under the same reaction conditions, PMo only gives a sulfide conversion of 58%. In all experiments performed, the synthesized catalyst showed more activity and selectivity in the diphenylsulfide oxidation to sulfoxide than the corresponding PMo, especially when vanadium was incorporated.



Scheme 1 Selective oxidation of sulfide to sulfoxide and/or sulfone

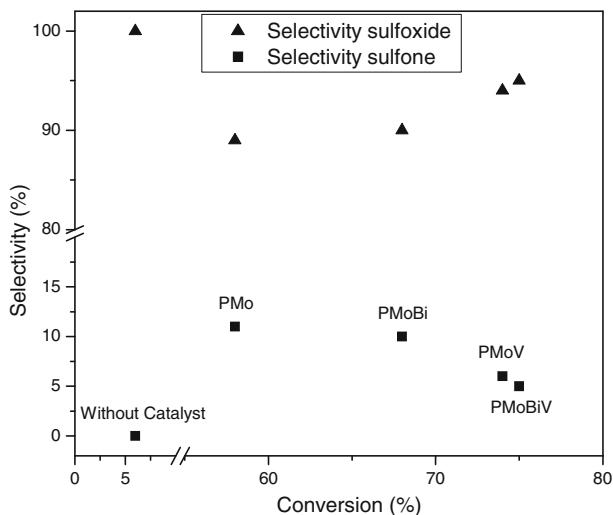


Fig. 4 Catalytic performance of different HPAs in diphenylsulfide oxidation. Sulfoxide and sulfone selectivity (%) versus sulfide conversion (%). Experimental conditions: bulk HPA (6 mg), 0.7 mmol of diphenylsulfide, H_2O_2 , 35% (w/v) (0.65 mmol, 0.075 mL), and 2 mL of ethanol, reaction for 7 h at 25 °C

The PMoV catalyst shows unique catalyst features for oxidation due to its bifunctional character, which arises because of the redox nature of Vanadium and the oxidation/acidic character of the molybdophosphoric acid [34]. As reported by Song et al. [1], the metal substitution may be modifying the energy and composition of the lowest unoccupied molecular orbital (LUMO) and consequently its redox properties. The substitution of vanadium ions into the molybdenum framework stabilizes the LUMOs because these orbitals derive in part from vanadium *d*-orbitals, which have been assumed to be more stable than those of Molybdenum and Tungsten. In this direction, Barteau et al. [29] reported that the absorption edge in the UV–visible spectrum of HPAs measures the energy required for ligand-to-metal charge transfer (LMCT). This represents the transfer of an electron from the highest occupied molecular orbital (HOMO) to the LUMO. Because the HOMO involves mostly the terminal oxygens, its energy is not greatly affected by changes in the HPA framework. However, the LUMO is greatly affected because it involves the bridging oxygen and the *d*-orbitals of the framework metals. Thus, changes in the absorption edge largely reflect changes in the LUMO [29]. The use of UV–visible spectroscopy of HPAs in solution could be a simple diagnosis of the redox properties.

Fig. 5 shows the correlation between the conversion (%) of diphenylsulfide and the adsorption edge of the HPA catalyst in solution. HPAs having adsorption edge energies below 2.31 eV displayed significant catalytic activity. As adsorption edge energies dropped from 2.31 to 2.26 eV with framework vanadium substitution into these Keggin HPAs, there was a general increase in sulfide conversion (Fig. 5).

Then, we performed the selective oxidation of diphenylsulfide to diphenylsulfone using an excess of H_2O_2 (35% (w/v), 0.7 mL, 6.6 mmol) at 50 °C. Under these conditions, it is possible to obtain diphenylsulfone selectively. All the doped catalysts presented a similar catalytic activity, which was higher than that of PMo. At short reaction times, when the PMoBi catalyst is used (Fig. 6), a 24% of sulfone selectivity is observed at 1 h, with a 100% of sulfide conversion. The sulfone selectivity for PMoV and PMoVBi catalysts is similar (30 and 35%, respectively), and for PMo it is only 12% under the same reaction conditions (Fig. 6). There is also a good correlation between sulfone selectivity (%) and the adsorption edge of the HPA catalyst in solution (Fig. 7).

Although HPA catalysts show a good performance in this reaction, the bulk HPAs are completely soluble in the reaction medium, and their isolation and reuse are difficult. In order to carry out the reaction under heterogeneous conditions, the more active HPAs were supported on amino-functionalized silica. Fig. 8 shows the results obtained using PMoV and PMoVBi supported on silica ($\text{SiO}_2\text{NH}_2\text{PMoV}$ and $\text{SiO}_2\text{NH}_2\text{PMoVBi}$), in the selective diphenylsulfide oxidation to diphenylsulfoxide at 25 °C. Silica-supported PMo was studied previously in the selective oxidation of sulfide to sulfones [35]. The PMoVBi catalyst supported on silica ($\text{SiO}_2\text{NH}_2\text{P-MoVBi}$) shows the best performance, sulfide conversion is low and sulfoxide selectivity is good. When this catalyst is used under the selective diphenylsulfide oxidation to sulfoxide conditions, a conversion of only 28% is observed at 27 h,

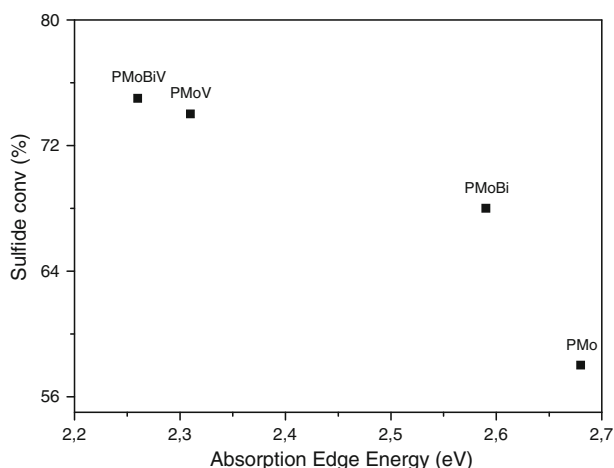


Fig. 5 Sulfide conversion (%) in the selective oxidation of diphenylsulfide to diphenylsulfoxide versus absorption edge energies for HPA ethanol solution. Experimental conditions: bulk HPA (6 mg), 0.7 mmol of diphenylsulfide, H_2O_2 , 35% (w/v) (0.65 mmol, 0.075 mL), and 2 mL of ethanol, reaction for 7 h at 25 °C

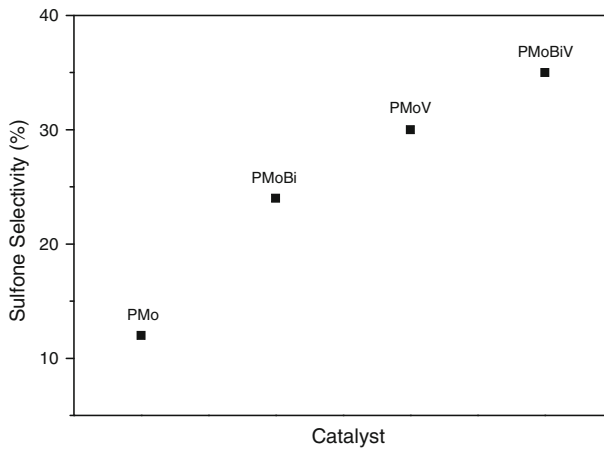


Fig. 6 Catalytic performance of different HPAs in diphenylsulfide oxidation. Sulfone selectivity (%). Experimental conditions: bulk HPA (12 mg), 1 mmol of diphenylsulfide, H_2O_2 , 35% (w/v) (6.6 mmol, 0.7 mL), and 4 mL of ethanol, reaction for 1 h at 50 °C. Sulfide conversion 1 h

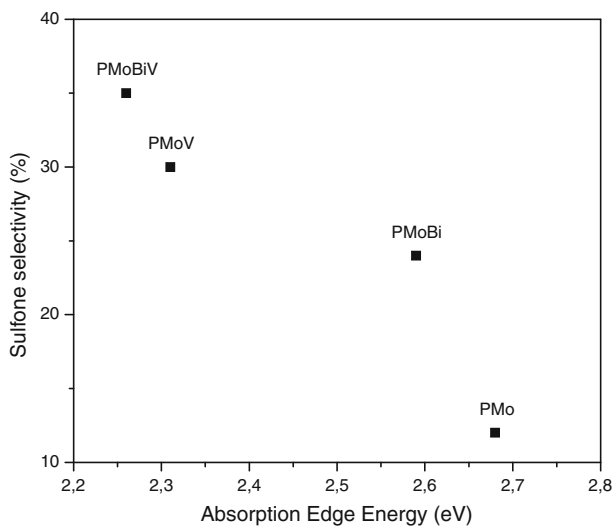


Fig. 7 Sulfone selectivity (%) in the oxidation of diphenylsulfide to diphenylsulfone versus absorption edge energies for HPA ethanol solution. Experimental conditions: bulk HPA (12 mg), 1 mmol of diphenylsulfide, H_2O_2 , 35% (w/v) (6.6 mmol, 0.7 mL), and 4 mL of ethanol, reaction for 1 h at 50 °C. Sulfide conversion 1 h

with a 55% of sulfoxide selectivity (Fig. 8). The catalytic activity of selected HPAs was tested at 50 °C using excess of H_2O_2 with the objective of obtaining diphenylsulfone selectivity. Both materials ($\text{SiO}_2\text{NH}_2\text{PMoV}$ and $\text{SiO}_2\text{NH}_2\text{PMoVBi}$) are excellent catalysts in the selective oxidation of diphenylsulfide to the corresponding sulfoxide or sulfone, depending on the reaction time. Fig. 9 shows the diphenylsulfide conversion versus the reaction time. The $\text{SiO}_2\text{NH}_2\text{PMoV}$ and

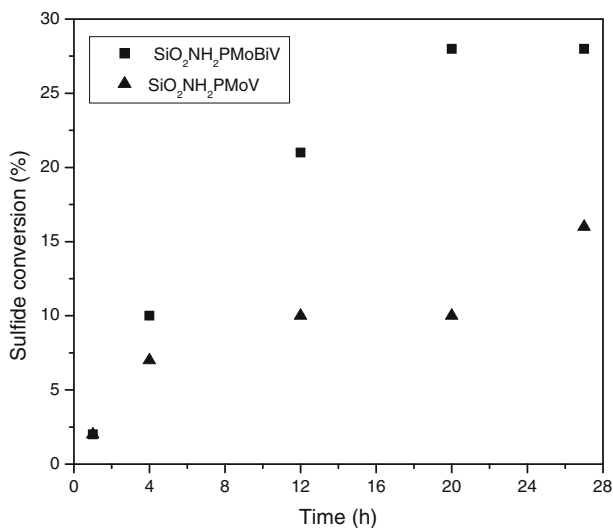


Fig. 8 Catalytic performance of SiO₂NH₂PMoBiV and SiO₂NH₂PMoV in the selective oxidation of diphenylsulfide. Sulfide conversion (%) versus time (h). Experimental conditions: the supported HPA (25 mg), 0.5 (93 mg) mmol of diphenylsulfide, H₂O₂, 35% (w/v) (0.65 mmol, 0.075 mL), and 2 mL of ethanol, reaction for 26 h at 25 °C

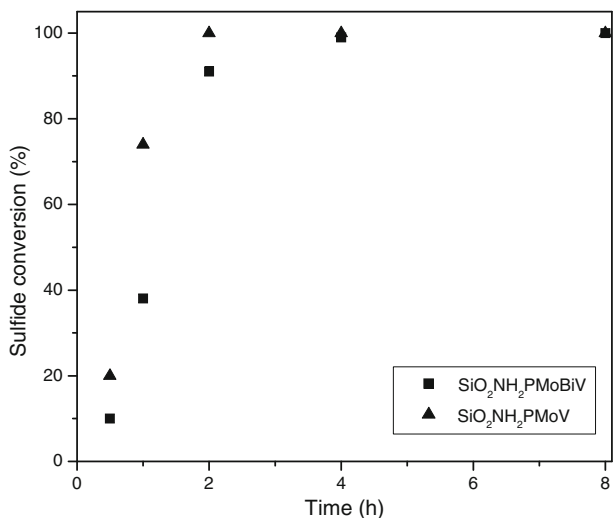


Fig. 9 Catalytic performance of SiO₂NH₂PMoBiV and SiO₂NH₂PMoV in the selective oxidation of diphenylsulfide. Sulfide conversion (%) versus time (h). Experimental conditions: the supported HPA (25 mg), 0.5 mmol of diphenylsulfide (93 mg), H₂O₂, 35% (w/v) (6.6 mmol, 0.375 mL), and 2 mL of ethanol, reaction for 8 h at 50 °C

SiO₂NH₂PMoVBi catalysts give a sulfide conversion and selectivity of 100% in a reaction time of 2 h and 4 h, respectively.

In addition, one of the main advantages of using supported solid catalyst in the liquid-phase reaction is the ease of separation and reuse of the catalyst in the

catalytic cycles. In this way, the catalyst ($\text{SiO}_2\text{NH}_2\text{PMoV}$) was separated by filtration, washed with ethanol, dried and then reused. No significant changes were observed after three catalytic cycles.

Conclusions

In this research, we report the preparation of doped Keggin structures with V, Bi and Bi–V, where Mo is partially replaced by those elements in molybdophosphoric acid (PMo). These catalysts were well characterized by means of FT-IR, ^{31}P -NMR, and UV–visible spectra. Mo, V and Bi amounts were estimated by ICP-AES analysis. In addition, the activities of the synthesized catalysts were evaluated in the selective oxidation of sulfides to sulfoxides/sulfones.

The correlation between catalytic oxidation performance (sulfide oxidation) and absorption edge energies of HPA catalysts demonstrated that the absorption edge energies could be utilized as a correlation parameter for the reduction potentials (oxidizing powers) of the HPA catalysts, and furthermore, as a probe of catalytic oxidation performance of the HPA catalysts.

Then, the two most active catalysts were immobilized on aminopropyl-functionalized silica. The materials prepared by the equilibrium adsorption technique ($\text{SiO}_2\text{NH}_2\text{PMoV}$ and $\text{SiO}_2\text{NH}_2\text{PMoVBi}$) were found to be efficient, ecofriendly and recyclable heterogeneous catalysts for the selective oxidation of diphenylsulfide to the corresponding sulfoxide/sulfone, under mild reaction conditions using aqueous hydrogen peroxide as the oxidant. The incorporation of V, Bi and Bi–V into the structure of PMo increases the catalytic activity.

Acknowledgments The authors thank E. Soto and D. Peña for their experimental contribution to the measurements of S_{BET} and GC, respectively. The authors thank CONICET, ANPCyT and UNLP for their financial support. AGS, PGV, HJT and GPR are members of CONICET.

References

1. Park D, Park P, Bang Y, Song I (2010) *Appl Catal A* 373:201–207
2. Romanelli G, Autino J (2009) *Mini Rev Org Chem* 6:359–366
3. Bennardi D, Romanelli G, Autino J, Pizzio L, Vázquez P, Cáceres C, Blanco M (2010) *React Kinet Mech Catal* 100:165–174
4. Romanelli G, Autino P, Vázquez P, Pizzio L, Blanco M, Cáceres C (2003) *Appl Catal A* 352: 208–213
5. Villabrille P, Romanelli G, Quaranta N, Vázquez P (2010) *Appl Catal B* 96:379–386
6. Sambeth J, Romanelli G, Autino J, Thomas H, Baronetti G (2010) *Appl Catal A* 378:114–118
7. Tundo P, Romanelli G, Vázquez P, Aricó F (2010) *Catal Commun* 11:1181–1184
8. Tundo P, Romanelli G, Vázquez P, Loris A, Aricó F (2008) *Synlett* 7:967–970
9. Villabrille P, Romanelli G, Vázquez P, Cáceres C (2008) *Appl Catal A* 334:374–380
10. Rao P, Venkateswara Rao K, Sai Prasad P, Lingaiah N (2010) *Catal Commun* 11:547–550
11. Kende A, Ebertino F (1984) *Tetrahedron Lett* 25:923–926
12. El Ali B, El-Ghanam A, Fettouhi M (2001) *J Mol Catal A* 165:283–289
13. Seki Y, Mizuno K, Misono M (2000) *Appl Catal A* 194:13–20
14. Trost B (1978) *Chem Rev* 78:363–382
15. Carreno M (1995) *Chem Rev* 95:1717–1760

16. Karami B, Ghoreishi-Nezhad M, Clark J (2005) *Org Lett* 8:625–628
17. Ogura K, Yahata N, Fujimori T, Fujita M (1990) *Tetrahedron Lett* 31:4621–4624
18. Ma Y, Liu R, Gong X, Li Z, Huang Q, Wang H, Song G (2006) *J Agric Food Chem* 54:7724–7728
19. Friedrich M, Meichle W, Bernhard H, Rihs G, Otto H (1996) *Archiv der Pharmazie* 329:361–370
20. Barrett A, Carr R, Attwood S, Richardson G, Walshe N (1986) *J Org Chem* 51:4840–4856
21. Varma R, Sain R, Meshram H (1997) *Tetrahedron Lett* 8:625–628 and references cited herein
22. Tajbakhsh M, Hosseinzadeh R, Shakoori A (2004) *Tetrahedron Lett* 45:1889–1893
23. Barton D, Li W (1998) *Tetrahedron Lett* 39:7075–7078
24. Iwahana T, Sakaguchi S, Ishii Y (1998) *Tetrahedron Lett* 39:9059–9062
25. Bonadies F, De Angelis F, Locati L, Scettri A (1996) *Tetrahedron Lett* 37:7129–7130
26. Kaczorowska K, Kolarska Z, Mitka K, Kowalski P (2005) *Tetrahedron* 61:8315–8327
27. Villabrille P, Romanelli G, Vázquez P, Cáceres C (2004) *Appl Catal A* 270:101–111
28. Tarlani A, Abedini M, Nemati A, Khabaz M, Amini M (2006) *J Colloid Interface Sci* 303:32–38
29. Barteau K, Lyons J, Song I, Barteau M (2006) *Top Catal* 41:55–62
30. Villabrille P, Romanelli G, Gassa L, Vázquez P, Cáceres C (2007) *Appl Catal A* 324:69–76
31. Vázquez P, Blanco M, Cáceres C (1999) *Catal Lett* 60:205–215
32. Vázquez P, Pizzio L, Cáceres C, Blanco M, Thomas H, Alesso E, Finkielstein L, Lantaño B, Moltrasio G, Aguirre J (2000) *J Mol Catal A* 161:223–232
33. Pizzio L, Romanelli G, Vázquez P, Autino J, Blanco M, Cáceres C (2006) *Appl Catal A* 308:153–160
34. Casarini D, Centi G, Jiro P, Lena V, Tvaruzkova Z (1993) *J Catal* 143:325–344
35. Palermo V, Vázquez P, Romanelli G (2009) *Phosphorus Sulfur Silicon Relat Elem* 12:3258–3268